The Journal of Laryngology & Otology (2012), **126**, *487–494*.
© JLO (1984) Limited, 2012
doi:10.1017/S0022215112000205

MAIN ARTICLE

Drug delivery in the nasal cavity after functional endoscopic sinus surgery: a computational fluid dynamics study

X B CHEN[1], H P LEE[1], V F H CHONG[2], D Y WANG[3]

Departments of [1]Mechanical Engineering, [2]Diagnostic Radiology, and [3]Otolaryngology, Yong Loo Lin School of Medicine, National University of Singapore, Singapore

Abstract

Background: Intranasal medication is commonly used for nasal disease. However, there are no clear specifications for intranasal medication delivery after functional endoscopic sinus surgery.

Methods: A three-dimensional model of the nasal cavity was constructed from computed tomography scans of an adult Chinese male who had previously undergone functional endoscopic sinus surgery in the right nasal cavity. Computational fluid dynamic simulations modelled airflow and particle deposition, based on discrete phase models.

Results: In the right nasal cavity, more particles passed through the upper dorsal region, around the surgical area, and streamed into the right maxillary sinus region. In the left cavity, particles were distributed more regularly and uniformly in the ventral region around the inferior turbinate. A lower inspiratory airflow rate and smaller initial particle velocity assisted particle deposition within the right maxillary sinus cavity. In the right nasal cavity, the optimal particle diameter was approximately 10^{-5} m for maxillary sinus cavity deposition and 3×10^{-6} m for bottom region deposition. In the right nasal cavity, altered back head tilt angles enhanced particle deposition in the top region of the surgical area, and altered right side head tilt angles helped enhance maxillary sinus cavity deposition.

Conclusion: This model indicates that a moderate inspiratory airflow rate and a particle diameter of approximately 10^{-5} m should improve intranasal medication deposition into the maxillary sinus cavity following functional endoscopic sinus surgery.

Key words: Drug Administration, Topical; Nasal Cavity; Paranasal Sinuses; Fluid Dynamics

Introduction

Nasal obstruction due to refractory chronic rhinosinusitis is most commonly treated using functional endoscopic sinus surgery (FESS).[1,2] Following FESS, chronic sinusitis is commonly treated using intranasal medication (e.g. corticosteroids) introduced into the sinus regions.[3] Correct delivery of intranasal corticosteroids is necessary in order to achieve optimal efficacy. However, the major factors determining deposition of intranasal corticosteroids within the paranasal sinuses (e.g. drug particle size, aerosol pressure and rate, and maxillary ostia size)[4] are still controversial.[5]

Various researchers have monitored drug deposition within the nose using *in vivo* human studies involving computed tomography (CT),[6] gamma scintigraphy with radio-enhanced particles,[7] and endoscopic video imaging using dyed test formulations.[8,9] However, these techniques are invasive and/or difficult to implement in live human subjects, and may involve radiation exposure or deposition of foreign particles within the lung.

Computational fluid dynamics modelling is an emerging technology which enables valid, accurate and straightforward assessment of particle deposition within the healthy nasal cavity.[10–16] This technology enables careful simulation and analysis of the effects of particle size, spray cone diameter and spray cone angle on the deposition of particles throughout the healthy nasal cavity.

However, to our best knowledge, such modelling has not been conducted within a nasal cavity which has undergone a FESS procedure.

In nasal cavities which have undergone FESS, the ostia may be enlarged and some ethmoid cells may have been removed. Therefore, it is possible that more airflow may be directed into the paranasal sinus cavities and the upper ethmoid and sphenoid sinus

Accepted for publication 18 July 2011 First published online 14 March 2012

https://doi.org/10.1017/S0022215112000205 Published online by Cambridge University Press

regions, which may affect the local deposition of intranasal medication.

Zhao *et al.*[17] conducted numerical airflow modelling of the maxillary sinus regions for pre- and post-FESS nasal cavities, but did not consider the effect of ethmoid cell removal.

More recently, Xiong *et al.*[18] constructed a post-FESS nasal cavity model, and found increased airflow into the sinus regions with reduced nasal resistance. However, their model employed virtual FESS based on modifications to a healthy nasal model, and only a laminar, low inspiration airflow rate was used.

Hence, the current study aimed to provide qualitative and quantitative information which could guide correct usage of intranasal medication in nasal cavities which have undergone conventional FESS procedures. Computed tomography scans were taken from an adult who had undergone FESS involving right maxillary sinus ostium enlargement and partial ethmoid and sphenoid sinus removal. Computational fluid dynamics modelling was then used to simulate the airflow and drug particle deposition within a nasal cavity model constructed using the CT scan images. Drug particle deposition along the left and right nasal cavity walls was recorded. We also present and discuss the effect of different particle diameters, inspiratory airflow rates and head tilt angles on maxillary sinus particle deposition.

Materials and methods

All the subject's personal identifiers were removed before data processing for the numerical study.

Institutional review board approval was obtained.

The patient was an adult Chinese male measuring 170 cm in height and 66 kg in weight, who had previously undergone conventional FESS on his right nasal cavity (Figure 1). Image acquisition, three-dimensional reconstruction, mesh grid formation and computational simulation followed the established techniques of our research group.[19–21] The CT scans were taken at 1.5 mm intervals, and the structures of the internal nasal cavity were confirmed using endoscopy and acoustic rhinometry measurements.

A three-dimensional image model (nasal cavity domain 76.14 cm^3, Figure 2), which included the surrounding air volume within 10 cm of the nostril, was reconstructed using several commercially available software packages.[19–21] A typical nasal cavity model included paranasal maxillary, ethmoid and sphenoid sinuses and comprised approximately 2.45 million tetrahedral cells, which was adequate to ensure insensitivity to mesh density (Figure 2).

For the computational fluid dynamic simulations, airflow was assumed to be incompressible and quasi-steady. The Reynolds averaged Navier–Stokes equation was solved with a $k-\omega$ model and a shear stress transport option for complex laminar–transitional–turbulent airflow treatments.[13,14,19–22] Constant flow rates of 9.4, 18.8, 28.2 and 37.6 l/min at the nasopharynx were applied successively in order to model different breathing states (e.g. calm inspiration and medium and strong sniffing).[10,12,15,22] At the nostril, the pressure inlet boundary condition was applied with zero gauge pressure (i.e. atmospheric pressure). A discrete phase model was used to study the gas–particle flow (Figure 3). The Euler–Lagrange approach was implemented using the Lagrangian discrete phase model in the Fluent 6.3 software package (ANSYS, Canonsburg, Pennsylvania, USA).[11,15,22] The dispersed phase computations were performed by tracking 10 000 particles through the initially solved airflow field. Other simulation assumptions were similar to those reported previously.[22] The effects of accretions

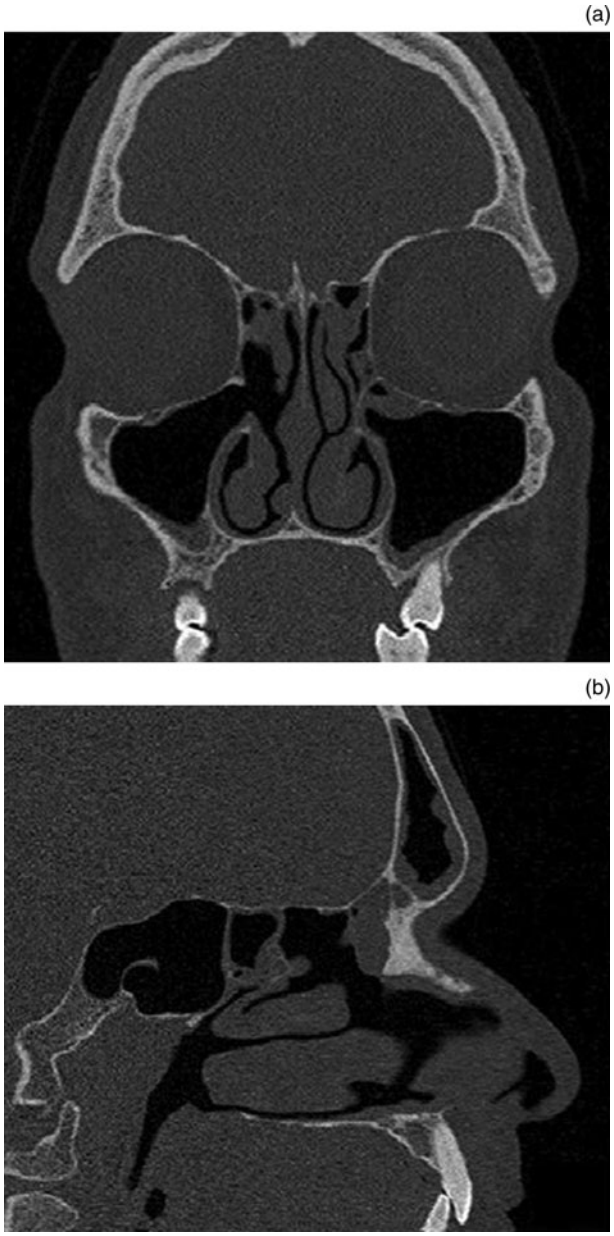


FIG. 1

Typical (a) coronal and (b) sagittal computed tomography scans of the nasal cavity of a patient following functional endoscopic sinus surgery.

https://doi.org/10.1017/S0022215112000205 Published online by Cambridge University Press

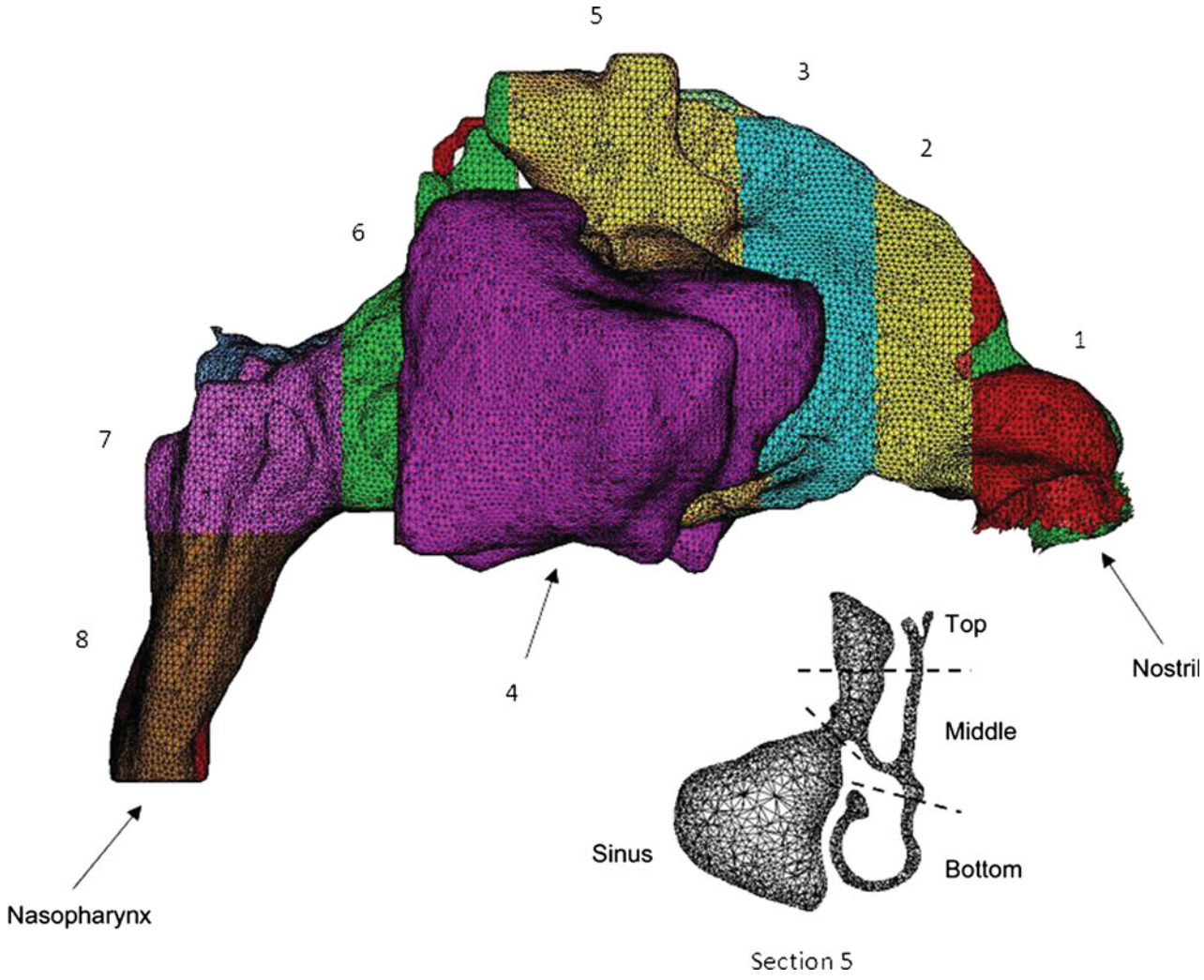


FIG. 2

Mesh illustration showing the left and right nasal cavities from the nostril to the nasopharynx, with differently coloured wall sections representing sections 1 to 8. The left and right maxillary sinuses (section 4) are shown as separate sections. Lower part shows division of section 5 into top, middle and bottom subsections.

and erosions were not considered, and particles were assumed to be trapped once they hit the nasal cavity wall.[11,15,22]

To analyse drug particle deposition in different regions of the nasal cavity wall, the wall was separated into eight sections, from the nostril to the nasopharynx (Figure 2). The maxillary sinus region was section four. In order to distinguish and investigate drug particle deposition in the upper ethmoid and sphenoid sinuses, section five was divided into top, middle and bottom subsections (see Figure 2). We investigated the effects of initial particle velocity, particle diameter, nasal flow rate, and back and right side head tilt angle (see Figure 3). Particle traces inside the left and right nasal cavities were simulated with a spray insertion angle of 55°, a spray cone angle of 79° and a spray penetration distance of 1 cm from the nostril, as suggested by Kimbell *et al.*[10] These parameters were fixed, while other factors were changed for the following computations.

Results

Figure 4 shows side and bottom views of the particle traces (colour-coded for particle residence time) for the left and right nasal cavities. For both cavities, it can be seen that the main particle streams were generally inside the main nasal cavity around the inferior turbinate in the ventral region. This was similar to reported particle streams within the healthy nasal cavity.[22] The residence time at the nasopharynx was relatively longer than that at the initial spray position. This was because of variation in local velocity, which was greater inside the cavity passageway than in those regions near the nasopharynx.[22,23]

However, in the right nasal cavity (Figure 4a) it can be seen that some particles entered into the upper ethmoid and sphenoid sinuses, in the dorsal region, and into the right maxillary sinus. Due to these particles' relatively small size, they followed the velocity streamlines where there were circular patterns (i.e. vortexes) within regions.[23] These particles stayed in these

https://doi.org/10.1017/S0022215112000205 Published online by Cambridge University Press

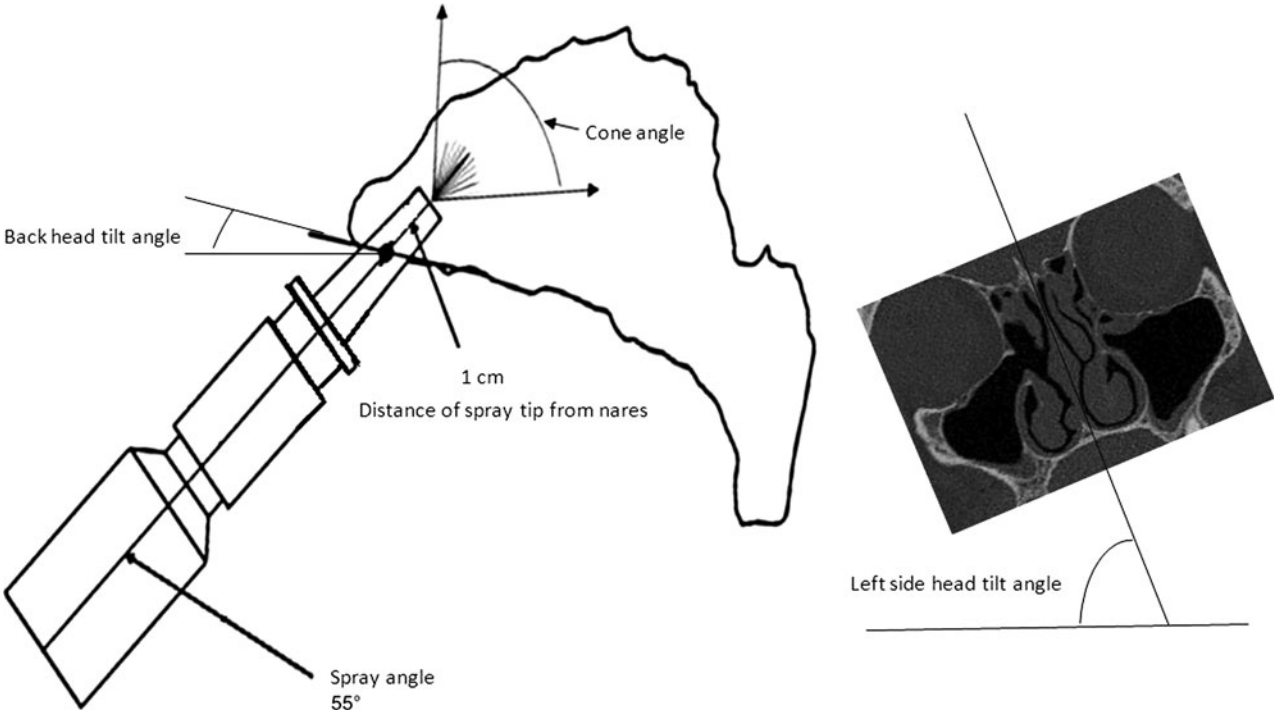


FIG. 3

Diagram plus coronal computed tomography scan, indicating the different geometric drug delivery parameters and positions of the nasal spray.

regions for a longer time, because of the abrupt decrease in velocity inside the wide sinus spaces.

In contrast, in the left nasal cavity (Figure 4b) fewer particles entered the maxillary and upper ethmoid and sphenoid sinuses, and particles were distributed much more uniformly. In the current model, only one particle entered the left maxillary sinus, but then circled back into the main nasal cavity.

Due to the previous FESS procedures in the right nasal cavity (Figure 1a), the maxillary sinus ostium was enlarged and parts of the ethmoid and sphenoid sinuses had been removed (Figure 1b). This could be expected to introduce a larger airflow from the main nasal cavity.[23] In contrast, in the left nasal cavity (Figure 1b) the original, small ostium of the left maxillary sinus, and the complex upper regions, were present

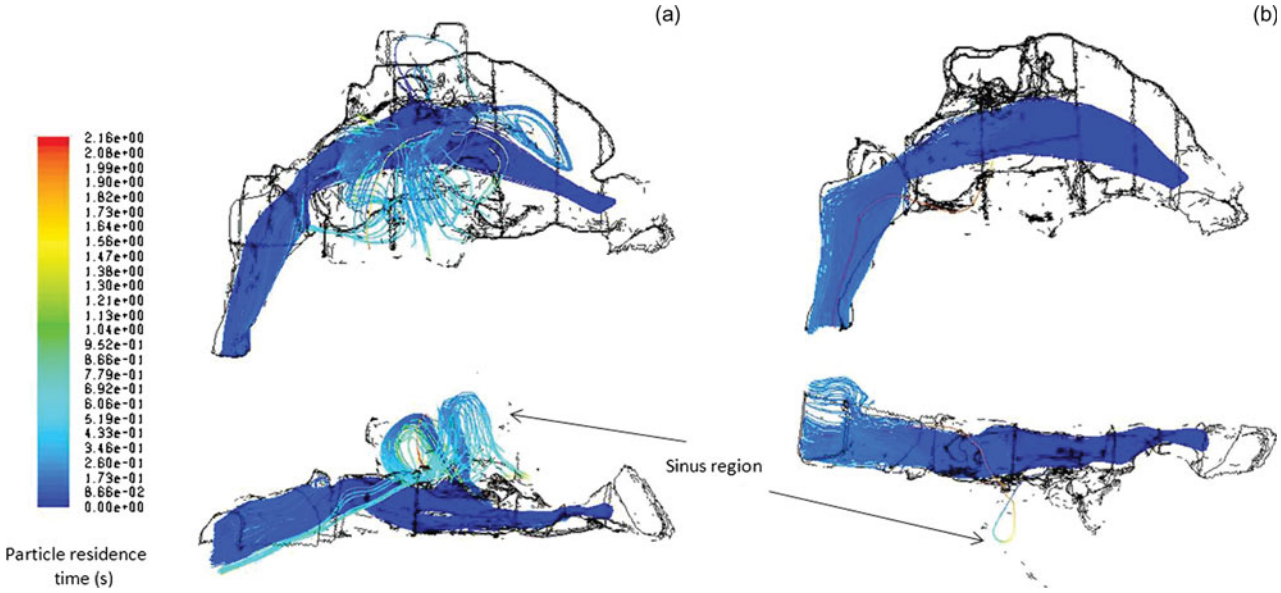


FIG. 4

Side (upper) and bottom (lower) views of particle traces (colour-coded for particle residence time) for the (a) right and (b) left nasal cavities. Initial particle velocity = 1 m/second, particle diameter = 10 μm, spray insertion angle = 55°, cone angle = 79°, nose flow rate = 18.8 l/min, back and right side head tilt angles = 0°.

https://doi.org/10.1017/S0022215112000205 Published online by Cambridge University Press

intact, and this helped to prevent most of the airflow (and thus drug particles) from entering these regions.[23]

Figure 5 shows particle deposition ratios, expressed as percentages, for the different sections of the left and right nasal cavity walls. Our research group has previously published a similar analysis of a healthy nasal cavity.[22] In both cavities, there was relatively greater particle deposition in section two due to this section's small cross-sectional area.[20–22] Particle deposition in the left nasal cavity was similar to that previously reported for healthy cases.[11,15,22] However, in the right nasal cavity the largest deposition ratio (23.21 per cent) was found at section five, around the FESS site; in contrast, relatively smaller deposition ratios were detected at sections six to eight, further downstream. The ratio of escaping particles was much higher for the right nasal cavity (40.78 per cent) than the left (4.60 per cent). As predicted previously, 1.54 per cent of total particles were found to deposit in the right maxillary sinus region. There was no particle deposition in the left maxillary sinus region.

Figure 6 shows particle deposition for the right nasal cavity section five and maxillary sinus regions, for different inspiratory airflow rates and initial particle velocities. It can be seen that a lower airflow rate and lower initial particle velocity resulted in increased deposition (from 0 per cent to a maximum of 3.51 per cent) at the top of section five and in the maxillary sinus (Figure 6a). However, these deposition changes were not as significant as those found at the middle subsection of section five (i.e. from 9.29 per cent to a maximum of 24.58 per cent; see Figure 6b). This was due to the fact that the internal main airflow (with peak velocity) brought together the main particle streams and resulted in local particle deposition in the upper middle passages around the inferior turbinate.[23]

Figure 6b also shows that changes in initial particle velocity did not lead to significant changes in deposition ratio in the bottom subsection of section five, and that the deposition ratio value decreased to nearly zero when the airflow rate was 9.4 l/min. This was because airflow velocity was relatively lower in the bottom subsection of section five,[23] and thus there

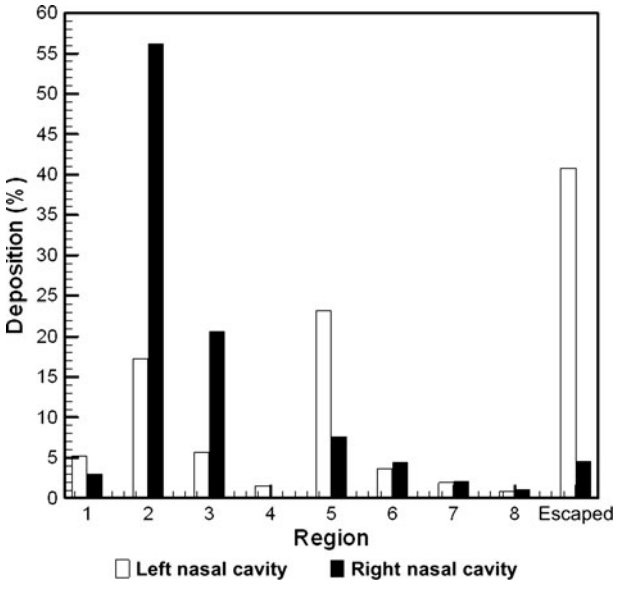


FIG. 5

Particle deposition in the different sections of the nasal cavity. Initial particle velocity = 1 m/second, particle diameter = 10 μm, spray insertion angle = 55°, cone angle = 79°, nose flow rate = 18.8 l/min, back and right side head tilt angles = 0°.

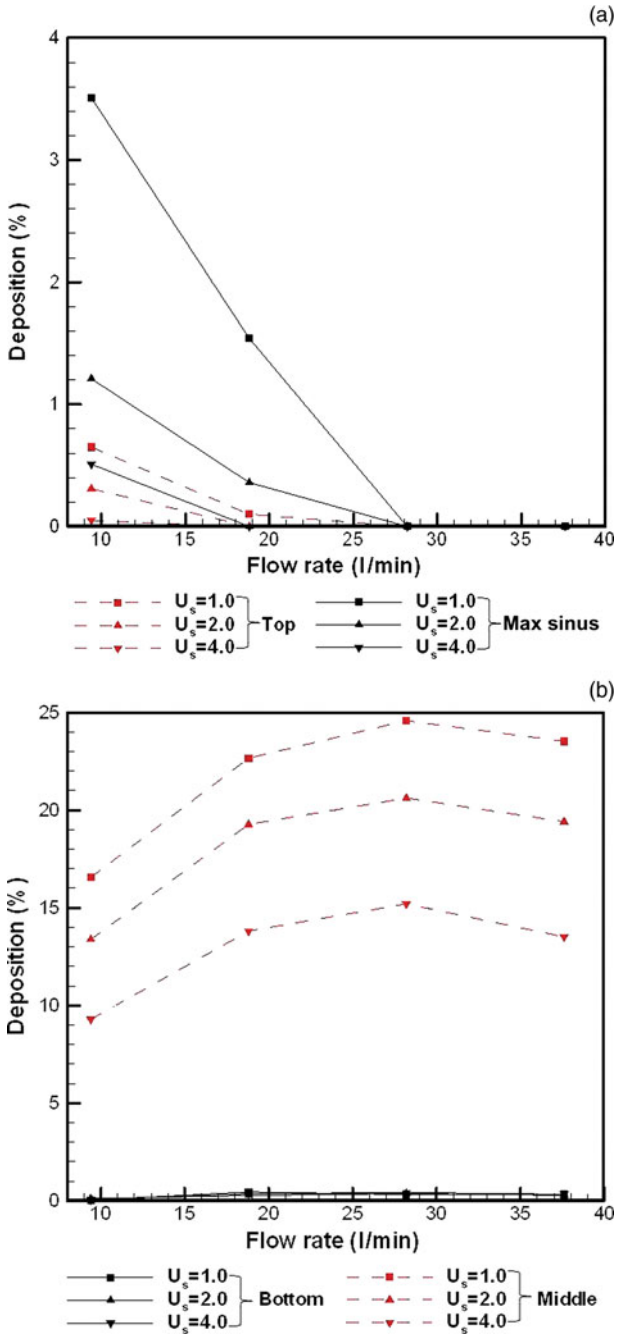


FIG. 6

Particle deposition in right nasal cavity (a) section five top subsection and maxillary sinus, and (b) section five middle and bottom subsections, for different flow rates and initial particle velocities (U_s). Particle diameter = 10 μm, spray insertion angle = 55°, cone angle = 79°, back and right side head tilt angles = 0°. Max = maxillary.

https://doi.org/10.1017/S0022215112000205 Published online by Cambridge University Press

was insufficient airflow to direct particles into this region. Figure 6b also shows that a constant initial particle velocity and an increasing airflow rate resulted in decreased deposition in the middle subsection of section five. This may be due to increasing deposition in the 'frontier' sections one to four with larger airflow rates over a short time period.

Similar to Figure 6b, Figure 7 shows that, in the middle subsection of section five, changes in particle diameter resulted in significant changes in deposition ratio. For particles 3 to 7×10^{-5} m in diameter, deposition increased as particle diameter decreased, whereas for particles smaller than 3×10^{-5} m in diameter deposition decreased as particle diameter decreased. Similarly, in the maxillary sinus region particles of approximately 10^{-5} m in diameter had the greatest deposition ratio. In contrast, in the bottom subsection of section five the optimal diameter was approximately 3×10^{-6} m. However, in the top subsection of section five the effect of particle diameter on deposition was not noticeable.

Tables I and II show that, in the absence of airflow (i.e. flow of 0 l/min), different back and right side head tilt angles produced only slight differences in deposition in section five of the right nasal cavity. The presence of inspiratory airflow aided particle deposition in the section five region, with greatest deposition occurring with a moderate airflow rate (e.g. 9.4 l/min). The optimum airflow rate differed between the section five and maxillary sinus regions, and also between the top, middle and bottom subsections of section five.

Table I also shows that changes in back head tilt angle helped enhance particle deposition in the top subsection of section five, but did so more effectively with a lower airflow rate (at 9.4 l/min, a change in back head tilt angle from 0 to 90° increased the deposition ratio from 0.65 to 4.01 per cent, an approximately six-fold increase). Table II shows that changes in right side head tilt angle helped enhance particle deposition in the right maxillary sinus region. Such changes were much more effective with a lower airflow rate (at 9.4 l/min, a change in right side head tilt angle from 0 to 90° increased the deposition ratio from 3.51 to 7.19 per cent, an increase of more than 100 per cent); furthermore, these changes enabled a greater increase in particle deposition than did changes in particle diameter (which increased deposition from 0 to 1.54 per cent; see Figure 7).

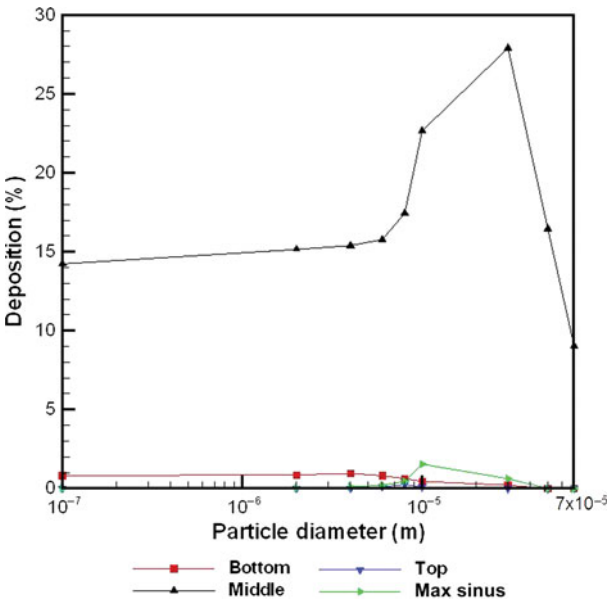


FIG. 7

Particle deposition in the section five (top, middle and bottom subsections) and maxillary sinus regions of the right nasal cavity for different particle diameters. Initial particle velocity = 1 m/s, spray insertion angle = 55°, cone angle = 79°, nose flow rate = 18.8 l/min, back and right side head tilt angles = 0. Max = maxillary.

TABLE I

PARTICLE DEPOSITION IN RIGHT NASAL CAVITY SECTION 5 AND MAXILLARY SINUS, BY AIRFLOW AND BACK HEAD TILT ANGLE

Airflow (l/min)	Back head tilt (°)	Section five PD (%)			Max sinus PD (%)
		Top	Middle	Bottom	
0	0	0.02	0.06	0.09	0
0	30	0.02	0.04	0.10	0
0	60	0.02	0.06	0.10	0
0	90	0.03	0.07	0.11	0
9.4	0	0.65	16.55	0.03	3.51
9.4	30	0.91	16.23	0.07	2.62
9.4	60	2.76	15.87	0.05	2.02
9.4	90	4.01	15.11	0.08	1.05
18.8	0	0.10	22.66	0.45	1.54
18.8	30	0.21	22.89	0.52	1.52
18.8	60	0.36	21.62	0.46	1.48
18.8	90	0.51	21.23	0.53	1.01

Initial particle velocity = 1 m/second, particle diameter = 10 μm, spray insertion angle = 55°, cone angle = 79°, right side head tilt angle = 0°. PD = particle deposition; max = maxillary

TABLE II

PARTICLE DEPOSITION IN RIGHT NASAL CAVITY SECTION 5 AND MAXILLARY SINUS, BY AIRFLOW AND RIGHT HEAD TILT ANGLE

Airflow (l/min)	R head tilt (°)	Section 5 PD (%)			Max sinus PD (%)
		Top	Middle	Bottom	
0	0	0.02	0.06	0.09	0
0	30	0.02	0.09	0.05	0
0	60	0.01	0.07	0.10	0
0	90	0.01	0.07	0.13	0
9.4	0	0.65	16.55	0.03	3.51
9.4	30	0.54	16.64	0.08	4.87
9.4	60	1.05	16.69	0.06	5.13
9.4	90	1.21	16.25	0.06	7.19
18.8	0	0.10	22.66	0.45	1.54
18.8	30	0.08	22.87	0.51	1.81
18.8	60	0.12	22.91	0.47	2.12
18.8	90	0.11	22.13	0.45	2.45

Initial particle velocity = 1 m/second, particle diameter = 10 μm, spray insertion angle = 55°, cone angle = 79°, back head tilt angle = 0°. R = right side; PD = particle deposition; max = maxillary

https://doi.org/10.1017/S0022215112000205 Published online by Cambridge University Press

Discussion

Following FESS for chronic sinusitis, corticosteroids are administered intranasally with the intention of delivering the drug particles into the paranasal sinuses.[3,4,24] However, there are few reported studies of how the physical properties of intranasal medication particles affect local deposition in the FESS region.[5]

Those authors who have reported deposition simulations in healthy nasal cavities have not included (or considered) the maxillary, ethmoid or sphenoid sinuses in their models.[10–16] This was due to the fact that there is negligible local airflow into these cavities. In these studies, particle deposition within the main nasal cavity was uniform and regular; deposition in this site is relatively easy to measure and describe using computational fluid dynamic tools.

In contrast, the post-FESS nasal cavity induces airflow into these sinus cavities due to enlarged sinus ostia and the absence of upper air cells and tissue (Figure 1). This increases the complexity of internal airflow patterns (with altered airflow circulation and the development of vortexes with changes in breathing state),[23] and thus affects local particle deposition.

We believe that the current model is the first reported attempt to investigate such abnormal particle deposition around the FESS site and within the sinus cavities, from a numerical viewpoint. The main objective of the current model was to characterise the effect of different particle properties and inspiratory factors on the local particle deposition at the FESS site and sinus cavities, and thus to enable optimisation of particle delivery.

Although the current model was based on a single human individual and thus may not be representative, our results still provide qualitative and quantitative information assisting the correct use of intranasal medication in patients undergoing FESS. We believe our findings will help improve the clinical efficacy of drug particle delivery, especially into the sinus regions. However, in order to make these results more relevant to the general population, similar studies are needed involving a number of post-FESS individuals with varying anatomy.

The current findings indicate that the optimal particle diameter for intranasal medication targeting the maxillary sinus region is approximately 10^{-5} m (see Figure 7). Hwang *et al.*[25] found that, for both normal and post-surgical nasal cavities, particles ranging from 0.9 to 1.1×10^{-5} m in diameter had superior deposition behaviour in the sinus regions. Hilton *et al.*[5] theoretically predicted that the best diameter range would be 0.3 to 1.0×10^{-5} m. The current predicted optimal diameter was within the above two groups' reported ranges. Hilton *et al.*[5] also reported that, in the maxillary sinus, improved particle deposition was obtained with smaller diameter particles. These authors used a nasal cavity model with FESS interventions to study the delivery of nebulised antibiotics. However, due to experimental restrictions, they reported an optimum mean diameter ranging from 0.67 to 0.99×10^{-6} m; in one additional case, the optimum diameter was 6×10^{-6} m. We compared the deposition results of these two group studies,[5,25] bearing in mind the fact that they may not have been thorough and complete surveys. In contrast, our computational fluid dynamics model enabled a numerical, quick, straightforward approach to investigating particle deposition in the sinus regions, for a wider range of particle diameters.

- **This study assessed drug particle deposition in normal and post functional endoscopic sinus surgery (FESS) nasal cavities, using a computational fluid dynamics model**
- **Airflow changes caused differing particle deposition in the two cavities, including sinus cavity deposition**
- **Particle deposition in the post-FESS maxillary sinus was greatest at low inspiratory airflow and low initial particle velocity**
- **Optimal particle diameter for local deposition was approximately 10^{-5} m for the maxillary sinus and 3×10^{-6} m for the base wall of the FESS section**

It should be noted that the current nasal cavity model incorporated FESS involving removal of the uncinate process. The preservation or removal of the uncinate process remains a controversial topic for FESS surgeons.[26] Following FESS procedures, post-operative infection most commonly involves non-colonising bacteria.[27] It has been proposed that the uncinate process may play a protective role, preventing deposition of bacteria and allergens. This theory may be supported by the current results, i.e. increased particle deposition in the sinus regions, which was more obvious with a lower inspiratory airflow rate.

Although not included in the current model, higher rates of maxillary sinus cilia motion may aid particle deposition, and may also affect local bacterial infection after FESS.[28]

The current findings also suggest that, in the sinus regions, the particle deposition ratio was larger when airflow was present rather than absent. A moderate airflow rate was optimal (see Tables I and II), which is consistent with findings for the healthy nasal cavity.[22,29]

Following FESS, patients who self-administer intranasal medication to treat chronic sinusitis should be advised to maintain a moderate airflow rate, and may also be best advised to change their head tilt angle, in order to maximise deposition of medication onto the walls of the maxillary, upper ethmoid and sphenoid sinuses. In order to maximise medication deposition on specific areas of the nasal cavity wall, the optimal head position and airflow rate should be used, and the medication particles should be of optimal diameter;

https://doi.org/10.1017/S0022215112000205 Published online by Cambridge University Press

however, these parameters will vary depending on individual nasal anatomy.

Conclusion

This computational study provides qualitative and quantitative information aiding optimisation of intranasal medication delivery for patients who have undergone FESS procedures. Findings include particle deposition distributions along the lateral walls of both nasal cavities, one of which had previously undergone FESS, for particles with diameters between 10^{-7} and 7×10^{-5} m, and for a variety of inspiratory airflow rates and initial particle velocities.

Patients who self-administer intranasal medication following a FESS procedure should use a moderate inspiratory airflow rate, and the medication particle diameter should ideally be approximately 10^{-5} m, in order to improve particle deposition into the maxillary sinus cavity around the FESS region. Although changes in head position significantly alter particle deposition, this is not clinically relevant as the best deposition ratio thus produced is still below 10 per cent.

Acknowledgement

The authors would like to acknowledge the financial support of an Academic Research Grant (T208A3103) from the Ministry of Education, Singapore.

References

1 Stammberger H, Posawetz W. Functional endosopic sinus surgery – concept, indications and results of the Messerklinger technique. *Eur Arch Otorhinolaryngol* 1990;**247**:63–76
2 Tan BK, Lane AP. Endoscopic sinus surgery in the management of nasal obstruction. *Otolaryngol Clin North Am* 2009;**42**:227–40
3 Vaughan WC, Carvalho G. Use of nebulized antibiotics for acute infections in chronic sinusitis. *Otolaryngol Head Neck Surg* 2002;**126**:558–68
4 Hyo N, Takano H, Hyo Y. Particle deposition efficiency of therapeutic aerosols in the human maxillary sinus. *Rhinology* 1989;**27**:17–26
5 Hilton C, Wiedmann T, Martin MS, Humphrey B, Schleiffarth R, Rimell F. Differential deposition of aerosols in the maxillary sinus of human cadavers by particle size. *Am J Rhinol* 2008;**22**: 395–8
6 Senocak D, Senocak M, Bozan S. Sinonasal distribution of topically applied particles: computerized tomographic detection and the effects of topical decongestion. *Otolaryngol Head Neck Surg* 2005;**133**:944–8
7 Homer JJ, Maughan J, Burniston M. A quantitative analysis of the intranasal delivery of topical nasal drugs to the middle meatus: spray versus drop administration. *J Laryngol Otol* 2002;**116**:10–13
8 Dowley AC, Homer JJ. The effect of inferior turbinate hypertrophy on nasal spray distribution to the middle meatus. *Clin Otolaryngol Allied Sci* 2001;**26**:488–90
9 Merkus P, Ebbens FA, Muller B, Fokkens WJ. The 'best method' of topical nasal drug delivery: comparison of seven techniques. *Rhinology* 2005;**43**:102–7
10 Kimbell JS, Segal RA, Asgharian B, Wong BA, Schroeter JD, Southall JP *et al*. Characterization of deposition from nasal spray devices using a computational fluid dynamics model of the human nasal passages. *J Aerosol Med* 2007;**20**:59–74
11 Inthavong K, Tian ZF, Tu JY, Yang W. Optimising nasal spray parameters for efficient drug delivery using CFD. *Comput Biol Med* 2008;**38**:713–26
12 Shi H, Kleinstreuer C, Zhang Z. Laminar airflow and nanoparticle or vapor deposition in a human nasal cavity model. *J Biomech Eng* 2006;**128**:697–706
13 Liu Y, Edgar AM, Gu JJ, Matthew RJ. Numerical simulation of aerosol deposition in a 3-D human nasal cavity using RANS, RANS/EIM, and LES. *J Aerosol Sci* 2007;**38**:683–700
14 Xi JX, Longest PW. Numerical predictions of submicrometer aerosol deposition in the nasal cavity using a novel drift flux approach. *Int J Heat Mass Transfer* 2008;**51**:5562–77
15 Inthavong K, Tian ZF, Li HF, Tu JY, Yang W, Xue CL *et al*. A numerical study of spray particle deposition in a human nasal cavity. *Aerosol Sci Technol* 2006;**40**:1034–45
16 Shanley KT, Zamankhan P, Ahmadi G, Hopke PK, Cheng YS. Numerical simulations investigating the regional and overall deposition efficiency of the human nasal cavity. *Inhal Toxicol* 2008;**20**:1093–100
17 Zhao K, Pribitkin EA, Cowart BJ, Rosen D, Scherer PW, Dalton P. Numerical modeling of nasal obstruction and endoscopic surgical intervention: outcome to airflow and olfaction. *Am J Rhinol* 2006;**20**:308–16
18 Xiong GX, Zhan JM, Jiang HY, Li JF, Rong LW, Xu G. Numerical flow simulation in the post-endoscopic sinus surgery nasal cavity. *Med Biol Eng Comput* 2008;**46**:1161–7
19 Chen XB, Lee HP, Chong VFH, Wang DY. Assessment of septal deviation effects on nasal air flow: a computational fluid dynamics model. *Laryngoscope* 2009;**119**:1730–6
20 Chen XB, Lee HP, Chong VFH, Wang DY. Impact of inferior turbinate hypertrophy on the aerodynamic pattern and physiological functions of the turbulent airflow – a CFD simulation model. *Rhinology* 2010;**48**:163–8
21 Chen XB, Leong SC, Lee HP, Chong VFH, Wang DY. Aerodynamic effects of inferior turbinate surgery on nasal airflow – a computational fluid dynamics model. *Rhinology* 2010;**48**:394–400
22 Chen XB, Lee HP, Chong VF, Wang DY. A computational fluid dynamics model for drug delivery in a nasal cavity with inferior turbinate hypertrophy. *J Aerosol Med Pulm Drug Del* 2010; **23**: 329–38
23 Chen XB, Lee HP, Chong VFH, Wang DY. Effects of functional endoscopic sinus surgery on nasal air flow – a computational fluid dynamics study. In: C.T. Lim, J.C.H. Goh. *6th World Congress on Biomechanics*, 1 – 6 August, 2010. Singapore: 1. Edition, Springer-Verlag, 2010
24 Moss RB, King VV. Management of sinusitis in cystic fibrosis by endoscopic surgery and serial antimicrobial lavage: reduction in recurrence requiring surgery. *Arch Otolaryngol Head Neck Surg* 1995;**121**:566–72
25 Hwang PH, Woo RJ, Fong KJ. Intranasal deposition of nebulized saline: a radionuclide distribution study. *Am J Rhinol* 2007;**20**:255–61
26 Nayak DR, Balakrishnan R. De novo bacterial reinfections after endoscopic sinus surgery: can uncinate process preservation surgeries prevent it? *Laryngoscope* 2005;**115**:928
27 Bhattacharyya N, Gopal HV, Lee KH. Bacterial infection after endoscopic sinus surgery: a controlled prospective study. *Laryngoscope* 2004;**114**:765–7
28 Bhattacharyya N. Response. De novo bacterial reinfections after endoscopic sinus surgery: can uncinate process preservation surgeries prevent it? *Laryngoscope* 2005;**115**:928–9
29 Schroeter JD, Kimbell JS, Asgharian B. Analysis of particle deposition in the turbinate and olfactory regions using a human nasal computational fluid dynamics model. *J Aerosol Med* 2006;**19**:301–13

Address for correspondence:
Dr De Yun Wang,
Department of Otolaryngology,
Yong Loo Lin School of Medicine,
National University of Singapore,
5 Lower Kent Ridge Road,
Singapore 119260

Fax: +65 67753820
E-mail: entwdy@nus.edu.sg

Dr X B Chen takes responsibility for the integrity of the content of the paper
Competing interests: None declared

https://doi.org/10.1017/S0022215112000205 Published online by Cambridge University Press